PHYSICAL REVIEW B **85**, 041201(R) (2012)

Orbital, charge, and spin couplings in $Ru_2^{5+}O_9$ dimers of $Ba_3CoRu_2O_9$

H. D. Zhou,[1,*] A. Kiswandhi,[1,2] Y. Barlas,[1] J. S. Brooks,[1,2] T. Siegrist,[1,3] G. Li,[1] L. Balicas,[1] J. G. Cheng,[4] and F. Rivadulla[5]

[1]*National High Magnetic Field Laboratory, Florida State University, Tallahassee, Florida 32306-4005, USA*

[2]*Department of Physics, Florida State University, Tallahassee, Florida 32306-3016, USA*

[3]*Department of Chemical and Biomedical Engineering, Florida State University, Tallahassee, Florida 32310, USA*

[4]*Texas Materials Institute, University of Texas at Austin, Austin, Texas 78712, USA*

[5]*Center for Research in Biological Chemistry, Physical-Chemistry Department, and Centro de Investigación en Química Biológica y Materiales Moleculares (CIQUS), University of Santiago de Compostela, 15782 Santiago de Compostela, Spain*

(Received 7 November 2011; published 9 January 2012)

The magnetic, transport, and structural properties of cold-pressed $Ba_3CoRu_2O_9$ show (i) an antiferromagnetic transition, (ii) a semiconductor-semiconductor electronic transition where the resistivity is dominated by the electron hopping between the $Ru_2^{5+}O_9$ dimers with itinerant Ru electrons at high temperatures, and (iii) a hexagonal to orthorhombic structural phase transition. All three transitions occur at 93 K and are related to the Ru^{5+} ions in the Ru_2O_9 dimers. The Ru-O bond distortion below 93 K further indicates a possible orbital ordering for Ru^{5+} ions in isolated Ru_2O_9 dimers, which accounts for the strong orbital, charge, and spin couplings.

DOI: 10.1103/PhysRevB.85.041201 PACS number(s): 75.25.Dk, 71.30.+h, 72.80.Ga

A fundamental question in physics concerns the interplay between the orbital and spin degrees of freedom, and if they exhibit coexisting ordered phases. The transition-metal oxides, which contain d electrons with partially filled t_{2g} or e_g orbitals, represent a major category of orbital ordering (OO) materials.[1–7] Lifting the degeneracy of these orbitals leads to a site-selective orbital occupation or an orbitally ordered phase. Since this ordered phase is related to exchange interactions, a spin order usually occurs simultaneously. Ruthenium-based oxides are good examples which exhibit strong spin and orbital coupling with 4d electrons. The OO transition in these ruthenates is usually accompanied by either a metal-insulator or a semiconductor-semiconductor electronic transition, indicating that the charge degrees of freedom also play an important role. Examples include $La_4Ru_2O_{10}$,[8,9] Ca_2RuO_4,[10–13] and pyrochlore $Tl_2Ru_2O_7$.[14,15]

So far, however, studies of orbital, charge, and spin couplings in the ruthenates have focused on materials containing Ru^{4+} ions. Studies on ruthenates containing Ru^{5+} ions have been limited by the difficulty in oxidizing Ru to be pentavalent. The Ru^{5+} ($4d^3$ $S = 3/2$) has three t_{2g} electrons which are degenerate, in contrast to Ru^{4+} ($4d^4$). The studied Ru^{5+} systems include R_3RuO_7 (R: La, Pr, Nd, and Gd),[16] $Ba_5Ru_2Cl_2O_9$,[17] Li_3RuO_4,[18] and the pyrochlore $Hg_2Ru_2O_7$.[19,20] $Hg_2Ru_2O_7$ shows a simultaneous magnetic and metal-insulator transition at ~107 K. Further studies suggest that a structural distortion is concomitant with both transitions, although it still remains unclear whether there is an OO transition associated with the Ru^{5+} ions.

Here, we turn our attention to another Ru^{5+} ruthenate, $Ba_3CoRu_2O_9$. This compound has the hexagonal barium titanate type of structure with $Ru_2^{5+}O_9$ structural dimers, made from face-sharing RuO_6 octahedra, interconnected by corner-sharing $Co^{2+}O_6$ octahedra [Fig. 1(a)]. Along the c axis, layers containing Ru_2O_9 dimers are separated by Co layers. Previously reported studies showed that this material is a semiconductor with an antiferromagnetic (AFM) transition at $T_N \sim 100$ K.[21,22] However, neutron measurements determined that, below T_N, the magnetic moment for Ru^{5+} is only 1.16 μ_B, which is certainly smaller than the expected $3\mu_B$ for $S = 3/2$. Also, whether there is a structural distortion at T_N, or the nature of the semiconducting phases at each side of this magnetic transition, remains unknown. In this Rapid Communication, we report the magnetization, transport, and structural properties of $Ba_3CoRu_2O_9$. Our results show that an AFM transition, a hexagonal-orthorhombic structural transition related with the distortion of the Ru-O bonds in the Ru_2O_9 dimers, and a semiconductor-semiconductor electronic transition related with a reduction in the number of charge carriers, all occur simultaneously at approximately $T^\star = T_N = 93$ K. We argue that these results present evidence for an OO state within the t_{2g} manifold of the Ru^{5+} ions, which accounts for the strong coupling observed among the orbital, charge, and spin degrees of freedom.

Cold-pressed pellets of polycrystalline $Ba_3CoRu_2O_9$ were prepared by a standard solid-state reaction.[23] The room-temperature x-ray diffraction (XRD) pattern of $Ba_3CoRu_2O_9$ shows a single phase with a hexagonal, $P6_3/mmc$, structure. The lattice parameters are $a = 5.7454(2)$ Å and $c = 14.1117(3)$ Å, similar to the reported data.[21,22] The dc magnetic susceptibility (χ) [Fig. 2(a)] shows a sharp drop below 100 K. The transition temperature $T_N = 93$ K is determined as the peak position of the $d\chi/dT$ vs T curve. The Curie-Weiss (CW) fitting to $\chi^{-1}(T)$ at high temperatures [Fig. 2(b)] yields the effective moment $\mu_{eff} = 7.6\mu_B$/formula or $4.4\mu_B$/Ru (or Co), if we assume Ru^{5+} and Co^{2+} contribute the same effective moment. This value is typical for d electron systems with $S = 3/2$, such as Co^{2+} ($3d^7$, $S = 3/2$) and Ru^{5+} ($4d^3$, $S = 3/2$).[24] The specific heat [Fig. 2(b)] also shows a peak at 93 K. The thermal conductivity $\kappa(T)$ [Fig. 2(c)] exhibits a relatively weak temperature dependence at high temperatures, followed by a suppression on approaching T_N from above. Below this temperature $\kappa(T)$ recovers the conventional behavior expected for a crystalline material, with a phonon peak at low temperatures. All measurements are consistent with a magnetic transition at $T_N = 93$ K. Previously reported neutron diffraction studies have shown that this corresponds to an AFM transition.[21,22] Below T_N, the measured magnetic moment is 2.84 μ_B for Co,

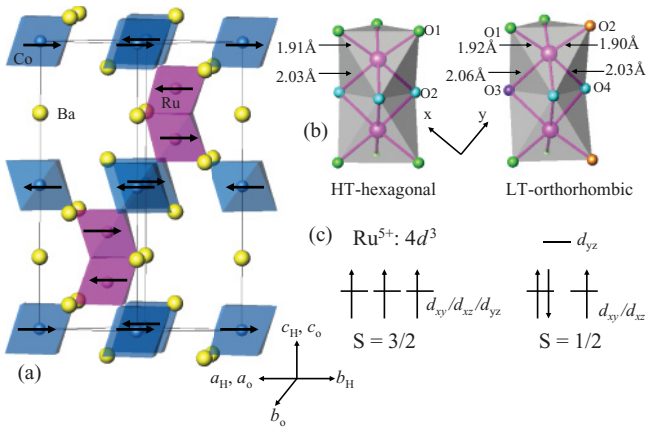

FIG. 1. (Color online) (a) Schematic representation of the Ru and Co octahedra packing in $Ba_3CoRu_2O_9$. The arrows show the schematic magnetic structure below T_N. (b) Ru-O distances in one Ru_2O_9 dimer with two face-shared RuO_6 octahedra for the high-temperature (HT)-hexagonal and the low-temperature (LT)-orthorhombic phases. (c) Schematic arrangements of the t_{2g} orbitals and spins for Ru^{5+} ($4d^3$) ions.

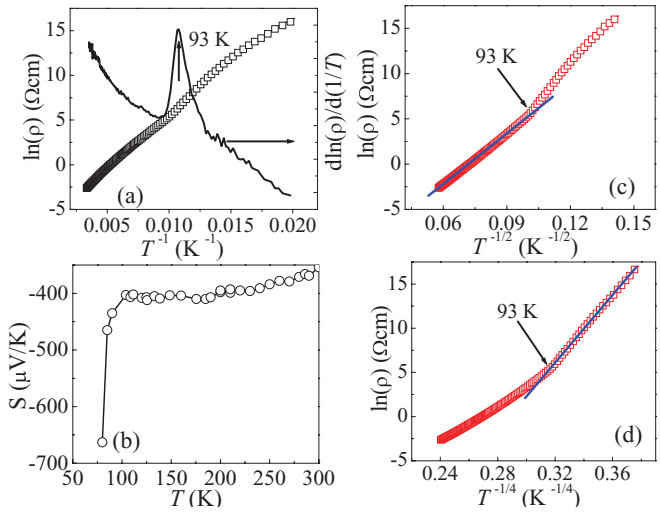

FIG. 3. (Color online) (a) $\ln(\rho)$ vs T^{-1} and $d\ln(\rho)/d(1/T)$ vs T^{-1} curves. (b) Temperature dependence of thermoelectric power. (c) $\ln(\rho)$ vs $T^{-1/2}$ curve. (d) $\ln(\rho)$ vs $T^{-1/4}$ curve. In (c) and (d) the open square is the experimental data and the solid lines are linear fittings.

which is consistent with three unpaired spins for Co^{2+}. On the other hand, the measured magnetic moment is 1.16 μ_B for Ru, which is smaller than $3\mu_B$ expected for Ru^{5+} ($S = 3/2$) ions,[21,22] but close to $1\mu_B$ expected for $S = 1/2$. This change from $S = 3/2$ (shown by CW fitting) above T_N to $S = 1/2$ below T_N for Ru^{5+} implies that two of the electrons form a singlet state in one of the orbitals, resulting from the lifting of the orbital degeneracy, as expected within an OO scenario.

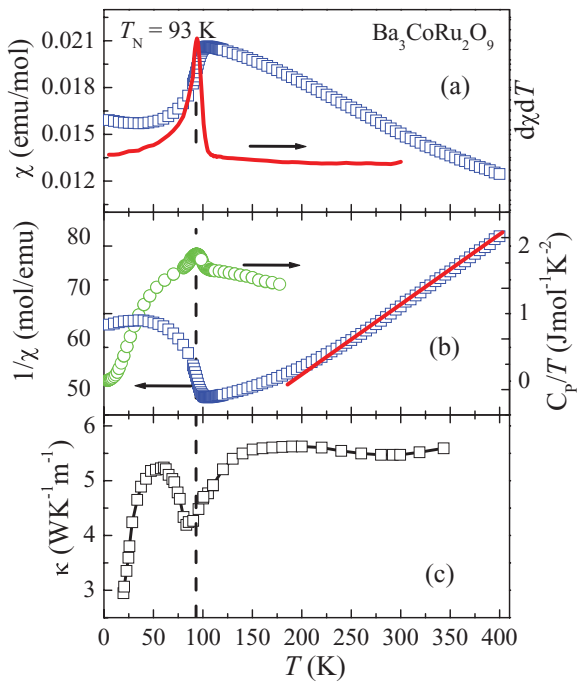

FIG. 2. (Color online) (a) Temperature dependencies of the dc magnetic susceptibility (χ) and its derivative for $Ba_3CoRu_2O_9$. (b) $1/\chi$ vs T and C_P/T vs T curves. The open square is the experimental data for $1/\chi$ and the solid line is the Curie-Weiss fitting. (c) Temperature dependence of the thermal conductivity.

The resistivity (ρ) shows semiconducting behavior below room temperature for $Ba_3CoRu_2O_9$. The $\ln(\rho)$ vs T^{-1} curve [Fig. 3(a)] shows a slope change at ~93 K. Moreover, the $d\ln\rho/d(1/T)$ vs T^{-1} curve shows a peak at ~93 K, which usually indicates an electronic transition. At the same time, thermoelectric power [$|S(T)|$, Fig. 3(b)] increases dramatically with decreasing temperature below 93 K, suggesting a sudden reduction in the number of charge carriers. Earlier studies of the resistivity on this material do not show evidence for an electronic transition at ~93 K. Furthermore, the reported value of the resistivity is significantly larger than our value at high temperatures, at $T = 300$ K, $\rho \approx 3$–4 Ω cm for the reported data,[25] orders of magnitude larger than our value of 0.07 Ω cm. The $\ln(\rho)$ vs T^{-1} curve does not show a perfect linear behavior, indicating that a single activation energy does not describe the resistivity over the entire temperature range. On the other hand, as shown in Fig. 3(c), the resistivity above 93 K is well described by a $\ln(\rho) \propto T^{-1/2}$ behavior. Below 93 K, the resistivity deviates from the $T^{-1/2}$ behavior and can be best described as $\ln(\rho) \propto T^{-1/4}$ [Fig. 4(d)]; this slope change again indicates an electronic transition.

In $Ba_3CoRu_2O_9$, the Co-Co (5 Å) distance is too large to allow orbital bonding or sharing electrons, therefore the $3d$ electrons of Co should remain localized. The Ru-Ru distance (2.6 Å), however, is short enough to allow orbital overlap and strong hybridization, which suggests that the $4d$ electrons could be shared within the Ru_2O_9 dimers. Since these dimers are disconnected by the localized Co layers, the bulk crystal structure is semiconducting. Above $T^\star$ the conduction mechanism results from the tunneling of carriers among the isolated Ru_2O_9 dimers. One can then model the transport in this material through a network of metallic Ru_2O_9 dimers on a regular lattice embedded in a dielectric medium. The transport of electrons from the Ru_2O_9 dimers requires a small charging energy $E_c = (e^2/d)F(s/d)$, where d is the size of the cluster, s is the distance between the grains involved in the

transport, and F is some geometrical function which depends on the distribution of the Ru_2O_9 dimers. The conductivity above the transition is then given as a compromise between the wave-function overlap $\exp[-2\alpha s]$ and the activation behavior $\exp[-E_c/(k_\beta T)]$,

$$\sigma = \sigma_0 \int_0^\infty ds \exp\left[-2\alpha s - \frac{E_c}{k_\beta T}\right], \qquad (1)$$

where $\alpha = [2m\phi/\hbar^2]^{1/2}$, with m denoting the electron mass and ϕ the effective barrier height. Since we are in a homogenous system the condition s/d is trivially satisfied and leads to the constraint $sE_c = \text{const}$. Physically this corresponds to the fact that the charging energy decreases with increasing distance. With this condition the integral can be evaluated by the method of steepest descents giving $\sigma = \sigma_0' \exp[-(T_0/T)^{1/2}]$, with $T_0 = 2\sqrt{C/k_\beta}$ and $C = \alpha s E_c$. It is also observed that the resistivity is sensitive to the applied electric field as the proposed model would suggest (see the Supplemental Material).[26] These behaviors are similar to the hopping transport seen in granular materials with metallic clusters embedded in a dielectric medium.[27,28] Above $T^\star$ the nearly temperature-independent thermoelectric power can be calculated using Onsager relations:

$$S = \frac{\Pi}{T} \propto \frac{1}{eT} N(\epsilon_F)[\Delta_{\text{eff}}(T)]^2 = \frac{k_\beta^2}{e} N(\epsilon_F) T_0, \qquad (2)$$

where Π is the Peltier heat and Δ_{eff} is the characteristic width in energy of the electron responsible for heat transport, which is given by $\exp[-\Delta_{\text{eff}}/(k_\beta T)] = \exp[-(k_\beta\sqrt{T_0 T})/(k_\beta T)]$. This further indicates that the thermoelectric power is dominated by the charge carriers and the sharp increase of $|S(T)|$ below $T^\star$ possibly corresponds to a reduction in itinerant carriers.

As shown above, both magnetic and electronic transitions occur at 93 K and are related to the Ru^{5+} ions in Ru_2O_9 dimers, which prompts the search for a concurrent structural transition. Earlier reported structural studies of this compound show contradicting results.[21,22] When our as-prepared $Ba_3CoRu_2O_9$ samples are cooled below 93 K, the XRD pattern begins to change, including the sudden increase in the width of the major Bragg peaks and the splitting of the peaks at high values of 2θ. Figures 4(a) and 4(b) show two XRD patterns at approximately $2\theta = 31.2^\circ$ and 90.5°. The single strongest peak at $\sim 31.2^\circ$ at 100 K shows an increased width and tends to split into two peaks at 85 K below $T^\star$; similarly, the two peaks at $\sim 90.5^\circ$ at 100 K split into three peaks at 85 K. This behavior indicates a structural phase transition at ~ 93 K. Above 93 K the XRD pattern can be well fit with the hexagonal structure $P6_3/mmc$ (HT phase), whereas below 93 K the patterns can be well fit with the orthorhombic structure $Cmcm$ (LT phase) with a lower symmetry with respect the hexagonal phase using a primitive unit cell having $a_{\text{ortho}} \sim a_{\text{hex}}$, $b_{\text{ortho}} \sim \sqrt{3} b_{\text{hex}}$, $c_{\text{ortho}} \sim c_{\text{hex}}$. As shown in Figs. 4(c)–4(e), below 93 K both a and c increase while b decreases with decreasing temperature. The calculated volume increases with decreasing temperature below 93 K, which shows a negative thermal expansion. Here the volume of the LT phase is calculated as the same unit cell as the HT phase for comparison. This abnormal negative thermal expansion also indicates that the transition for $Ba_3CoRu_2O_9$ is not only a simple AFM transition but also involves an electronic transition.

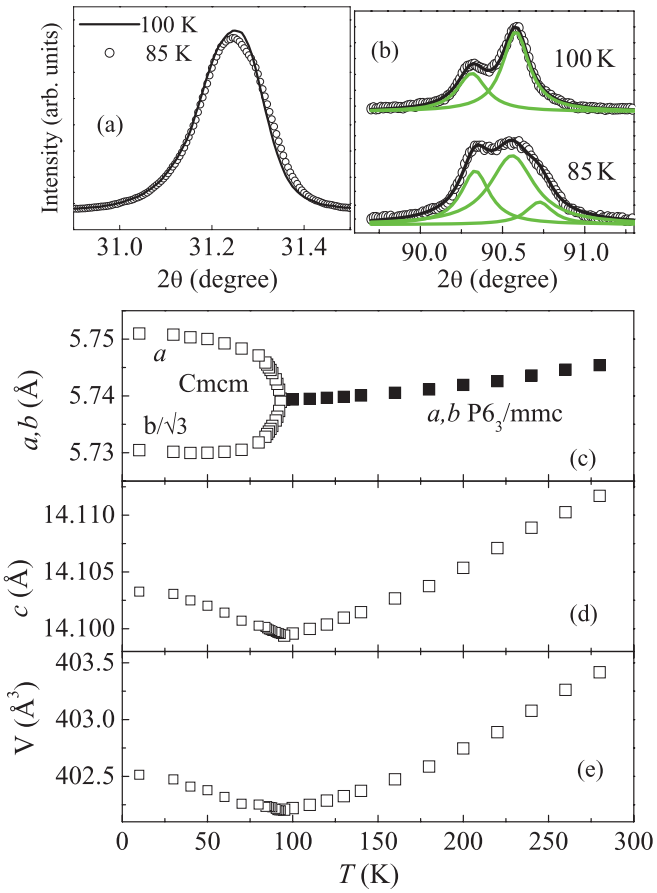

FIG. 4. (Color online) XRD scans at different temperatures for peaks at $\sim 2\theta$ as (a) 31.2° and (b) 90.5°. In (b) circles are experimental data, green (gray) lines are Lorentzian fittings, and black lines are the total fittings. Temperature dependencies of (c) lattice parameter a and b; (d) lattice parameter c; (e) volume.

The structural distortion is accompanied by a distortion of the RuO_6 octahedra in the Ru_2O_9 dimers. The previously reported neutron powder diffraction data[21,22] shows that, at room temperature, there are three short Ru-O1 bonds and three long Ru-O2 bonds, as shown in Fig. 1(b). The long Ru-O2 bonds extend to the O in the shared face between octahedra, due to the repulsion of the Ru^{5+} ions. Below $T^\star$, due to the structural distortion, there are now four types of Ru-O bonds [Fig. 1(b)].[21] The changes in the length of the long Ru-O3 and Ru-O4 bonds are not only due to the structural distortion but also due to the repulsion between Ru^{5+} ions. On the other hand, the change in the length of the short Ru-O1 and Ru-O2 bonds reflects the effect of the structural distortion. The three equivalent short Ru-O1 bonds at room temperature now change to two long Ru-O1 bonds (1.92 Å) and one short Ru-O2 bond (1.90 Å) in the LT phase.[21] This 1% difference in the bond length between Ru-O1 and Ru-O2 bonds below $T^\star$, which is related to a structural distortion, gives a strong indication of a possible orbital ordering transition of Ru orbitals. Because of the minimized repulsion between Ru d and O p orbitals, the shortest Ru-O2 bond is expected to lie along the axes of

unoccupied orbitals. Here we select the x axis of Ru in the LT phase along one of the long Ru-O1 bonds and the y axis to be along the short Ru-O2 bond. The compression of Ru-O2 bond length along the y axis will occur when the d_{yz} orbitals are unoccupied. Therefore, the distortion of the RuO_6 octahedra in a Ru_2O_9 dimer reflects a decreased orbital occupancy of d_{yz} orbitals and an increased occupancy of the d_{xz} or d_{xy} orbitals in the LT phase.

This OO scenario can consistently explain the strong coupling observed between the orbital, charge, and spin degrees of freedom for $Ba_3CoRu_2O_9$. Above $T^\star$ in the paramagnetic region, Ru^{5+} has three electrons to fill three degenerate t_{2g} orbitals based on the Hund's rule and gives $d^1_{xz}d^1_{yz}d^1_{xy}$ [see Fig. 1(c)]. Below $T^\star$, the compression of Ru-O bonds along the y axis destroys this configuration of the t_{2g} orbitals by inducing a gap which results in lifting the d_{yz} orbital to a higher-energy level than that of d_{xz} and d_{xy} orbitals. Therefore the electron configuration is adjusted to $d^2_{xz}d^1_{xy}$ or $d^1_{xz}d^2_{xy}$, as shown in Fig. 1(c). This configuration gives one unpaired spin ($S = 1/2$), which explains the measured $1\mu_B$ magnetic moment in the LT phase. Simultaneously, the depopulation of one electron from the d_{yz} orbital to d_{xz} or d_{xy} orbitals can suppress the itinerant character of the electrons in the Ru_2O_9 dimers or the number of charge carriers, which is manifested by the deviation of the resistivity from $\ln(\rho) \propto T^{-1/2}$ behavior and the sudden increase in the absolute value of the thermoelectric power below $T^\star$. At this stage electrons in the Ru^{5+} become localized and variable range hopping becomes the primary conduction mechanism, as indicated by the exponent $\beta = 1/4$. Moreover, orbital fluctuations, which usually occur at high temperatures above the OO transition could suppress the coherence among phonons and lead to the anomalous temperature dependence or glassylike thermal conductivity.[29–31]

Previously studied OO ruthenates have focused mainly on layered perovskite structures with corner-shared RuO_6 octahedra such as $La_4Ru_2O_{10}$ and Ca_2RuO_4, or a pyrochlore structure such as $Tl_2Ru_2O_7$ and $Hg_2Ru_2O_7$. Distinct from these examples, the possible OO transition for Ru^{5+} ions in $Ba_3CoRu_2O_9$ occurs in isolated Ru_2O_9 clusters with face-shared RuO_6 octahedra. This unique case greatly enriches the complex physics of orbital, charge, and spin couplings in transition-metal oxides.

This work is supported by NSF-DMR-0654118 and the State of Florida. J.S.B. and A.K. acknowledge support from NSF-DMR-1005293.

*zhou@magnet.fsu.edu

[1] G. Khaliullin, Prog. Theor. Phys. Suppl. **160**, 155 (2005).
[2] C. Ulrich, G. Khaliullin, S. Okamoto, M. Reehuis, A. Ivanov, H. He, Y. Taguchi, Y. Tokura, and B. Keimer, Phys. Rev. Lett. **89**, 167202 (2002).
[3] M. Mochizuki and M. Imada, Phys. Rev. Lett. **91**, 167203 (2003).
[4] Y. Ren, T. T. M. Palstra, D. I. Khomskii, E. Pellegrin, A. A. Nugroho, A. A. Menovsky, and G. A. Sawatzky, Nature (London) **396**, 441 (1998).
[5] C. Ulrich, G. Khaliullin, J. Sirker, M. Reehuis, M. Ohl, S. Miyasaka, Y. Tokura, and B. Keimer, Phys. Rev. Lett. **91**, 257202 (2003).
[6] J. B. Goodenough and J. S. Zhou, J. Mater. Chem. **16**, 2394 (2007).
[7] S. H. Lee, H. Takagi, D. Louca, M. Matsuda, S. Ji, H. Ueda, Y. Ueda, T. Katsufuji, J. H. Cheung, S. Park, S. W. Cheong, and C. Broholm, J. Phys. Soc. Jpn. **79**, 011004 (2010).
[8] H. Wu, Z. Hu, T. Burnus, J. D. Denlinger, P. G. Khalifah, D. G. Mandrus, L. Y. Jang, H. H. Hsieh, A. Tanaka, K. S. Liang, J. W. Allen, R. J. Cava, D. I. Khomskii, and L. H. Tjeng, Phys. Rev. Lett. **96**, 256402 (2006).
[9] P. Khalifah, R. Osborn, Q. Huang, H. W. Zandbergen, R. Jin, Y. Liu, D. Mandrus, and R. J. Cava, Science **297**, 2237 (2002).
[10] G. Cao, S. McCall, V. Dobrosavljevic, C. S. Alexander, J. E. Crow, and R. P. Guertin, Phys. Rev. B **61**, R5053 (2000).
[11] S. Nakatsuji and Y. Maeno, Phys. Rev. Lett. **84**, 2666 (2000).
[12] J. S. Lee, Y. S. Lee, T. W. Noh, S. J. Oh, J. Yu, S. Nakatsuji, H. Fukazawa, and Y. Maeno, Phys. Rev. Lett. **89**, 257402 (2002).
[13] J. H. Jung, Z. Fang, J. P. He, Y. Kaneko, Y. Okimoto, and Y. Tokura, Phys. Rev. Lett. **91**, 056403 (2003).
[14] H. Sakai, M. Kato, K. Yoshimura, and K. Kosuge, J. Phys. Soc. Jpn. **71**, 422 (2002).
[15] S. Lee, J. G. Park, D. T. Adroja, D. Khomskii, S.Streltsov, K. A. McEwen, H. Sakai, K. Yoshimura, V. I. Anisimov, D. Mori, R. Kanno, and R. Ibberson, Nat. Mater. **5**, 471 (2006).
[16] P. Khalifah, R. W. Erwin, J. W. Lynn, Q. Huang, B. Batlogg, and R. J. Cava, Phys. Rev. B **60**, 9573 (1999); M. Freamat, X. N. Lin, V. Durairaj, S. Chikara, G. Cao, and J. W. Brill, *ibid.* **72**, 014458 (2005); D. Harada, Y. Hinatsu, and Y. Ishii, J. Phys. Condens. Matter **13**, 10825 (2001); R. P. Bontchev, A. J. Jacobson, M. M. Gospodinov, V. Skumryev, V. N. Popov, B. Lorenz, R. L. Meng, A. P. Litvinchuk, and M. N. Iliev, Phys. Rev. B **62**, 12235 (2000).
[17] N. Tancret, P. Roussel, and F. Abraham, J. Solid State Chem. **177**, 806 (2004).
[18] A. Alexander, P. D. Battle, J. C. Burley, D. J. Gallon, C. P. Grey, and S. H. Kim, J. Mater. Chem. **13**, 2612 (2003).
[19] A. Yamamoto, Peter A. Sharma, Y. Okamoto, A. Nakao, H. A. Katori, S. Niitaka, D. Hashizume, and H. Takagi, J. Phys. Soc. Jpn. **76**, 043703 (2007).
[20] W. Klein, R. K. Kremer, and M. Jansen, J. Mater. Chem. **17**, 1356 (2007).
[21] P. Lightfoot and P. D. Battle, J. Solid State Chem. **89**, 174 (1990).
[22] J. T. Rijssenbeek, Q. Huang, R. W. Erwin, H. W. Zandbergen, and R. J. Cava, J. Solid State Chem. **146**, 65 (1999).
[23] J. S. Zhou, J. B. Goodenough, and B. Dabrowski, Phys. Rev. B **67**, 020404(R) (2003).
[24] R. L. Carlin, *Magnetochemistry* (Springer, Berlin, 1986), Chap. 4.
[25] J. T. Rijssenbeek, P. Matl, B. Batlogg, N. P. Ong, and R. J. Cava, Phys. Rev. B **58**, 10315 (1998).

[26]See Supplemental Material at http://link.aps.org/supplemental/10.1103/PhysRevB.85.041201 for *I-V* characteristics.

[27]P. Sheng, B. Abeles, and Y. Arie, Phys. Rev. Lett. **31**, 44 (1973).

[28]R. J. Kennedy, P. A. Stampe, E. Hu, P. Xiong, Stephan von Molnár, and Y. Xin, Appl. Phys. Lett. **84**, 2832 (2004).

[29]J. G. Cheng, Y. Sui, J. S. Zhou, J. B. Goodenough, and W. H. Su, Phys. Rev. Lett. **101**, 087205 (2008).

[30]J. Q. Yan, J. S. Zhou, J. B. Goodenough, Y. Ren, J. G. Cheng, S. Chang, J. Zarestky, O. Garlea, A. Llobet, H. D. Zhou, Y. Sui, W. H. Su, and R. J. McQueeney, Phys. Rev. Lett. **99**, 197201 (2007).

[31]B. Rivas-Murias, H. D. Zhou, J. Rivas, and F. Rivadulla, Phys. Rev. B **83**, 165131 (2011).